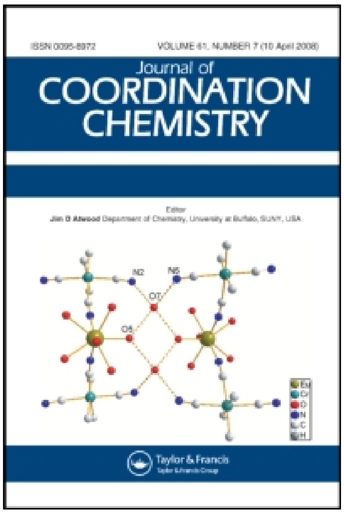

Journal of Coordination Chemistry
Publication details, including instructions for authors and subscription information:
http://www.informaworld.com/smpp/title~content=t713455674

Syntheses, structures, and properties of lead(II) and nickel(II) complexes with 3,5-di(1H-imidazol-1-yl)benzoate

Zhi Su[a]; Zhi-Bin Wang[a]; Wei-Yin Sun[a]
[a] Coordination Chemistry Institute, State Key Laboratory of Coordination Chemistry, School of Chemistry and Chemical Engineering, Nanjing National Laboratory of Microstructure, Nanjing University, Nanjing 210093, China

First published on: 30 November 2010

To cite this Article Su, Zhi , Wang, Zhi-Bin and Sun, Wei-Yin(2011) 'Syntheses, structures, and properties of lead(II) and nickel(II) complexes with 3,5-di(1H-imidazol-1-yl)benzoate', Journal of Coordination Chemistry, 64: 1, 170 — 178, First published on: 30 November 2010 (iFirst)

To link to this Article: DOI: 10.1080/00958972.2010.537332

URL: http://dx.doi.org/10.1080/00958972.2010.537332

Journal of Coordination Chemistry
Vol. 64, No. 1, 10 January 2011, 170–178

Taylor & Francis
Taylor & Francis Group

Syntheses, structures, and properties of lead(II) and nickel(II) complexes with 3,5-di(1H-imidazol-1-yl)benzoate

ZHI SU, ZHI-BIN WANG and WEI-YIN SUN*

Coordination Chemistry Institute, State Key Laboratory of Coordination Chemistry,
School of Chemistry and Chemical Engineering, Nanjing National Laboratory
of Microstructure, Nanjing University, Nanjing 210093, China

(*Received 26 July 2010; in final form 22 September 2010*)

Two new coordination polymers, $[Pb_2(L)_4(H_2O)] \cdot 4H_2O$ (**1**) and $[Ni(L)_2(H_2O)_2] \cdot 2H_2O$ (**2**), were obtained by hydrothermal reactions of 3,5-di(1H-imidazol-1-yl)benzoic acid (HL) with corresponding metal nitrates. In **1** and **2**, each L^- links two metals to form 1-D double strand chains, which are further connected by hydrogen bonds and π–π interactions to form 3-D frameworks. However, the coordination environments around Pb(II) in **1** and Ni(II) in **2** are different. One of the two imidazole groups of L^- does not take part in coordination in **1**, while the carboxylate of L^- in **2** is uncoordinated. The thermal stability of the complexes and the photoluminescence of **1** were investigated.

Keywords: Lead(II) complex; Nickel(II) complex; Hydrothermal reaction; Photoluminescence

1. Introduction

Coordination polymers have received considerable interest because of their intriguing topological architectures and interesting properties, as well as potential applications in catalysis, magnetism, luminescence, adsorption, and separation [1–5]. Tripodal ligands with imidazole or carboxylate groups are widely used in the construction of coordination polymers for their strong coordination ability [6–9]. However, ligands with both imidazole and carboxylate functional groups are rarely reported [10]. In this case, we designed and synthesized a ligand 3,5-di(1H-imidazol-1-yl)benzoic acid (HL), which has advantages compared to the ligands with only one functional group of imidazole or carboxylate [11, 12]. The ligand HL with both N and O coordination donors has strengthened coordination abilities, has more coordination modes to satisfy the geometric requirement of metal centers, and offers additional hydrogen bonding and π–π interactions to consolidate the crystal structure. In this study, HL was used to react with $Pb(NO_3)_2$ and $Ni(NO_3)_2 \cdot 6H_2O$ to investigate the effect of metal centers with

---

*Corresponding author. Email: sunwy@nju.edu.cn

Journal of Coordination Chemistry
ISSN 0095-8972 print/ISSN 1029-0389 online © 2011 Taylor & Francis
DOI: 10.1080/00958972.2010.537332

different coordination geometry on the structures of coordination polymers. The syntheses and crystal structures of $[Pb_2(L)_4(H_2O)] \cdot 4H_2O$ (**1**) and $[Ni(L)_2(H_2O)_2] \cdot 2H_2O$ (**2**) are reported herein. The thermal stability and photoluminescence of the complexes were also investigated.

2. Experimental

2.1. *Materials and methods*

All commercially available solvents and reagents are used as received. The HL was prepared according to the procedures reported previously [12]. Elemental analyses were performed on a Perkin-Elmer 240C elemental analyzer. IR spectra were recorded on Bruker Vector22 FT-IR spectrophotometer. Thermogravimetric analyses (TGA) were performed on a simultaneous SDT 2960 thermal analyzer under nitrogen with a heating rate of $10^\circ C\,min^{-1}$. Luminescence spectra for the powdered solid samples were measured at room temperature on an Aminco Bowman Series2 spectrofluorometer with a xenon arc lamp as the light source. In measurements of emission and excitation spectra the pass width is 5 nm. All measurements were carried out under the same experimental conditions.

2.2. *Syntheses of complexes*

2.2.1. $[Pb_2(L)_4(H_2O)] \cdot 4H_2O$ (1). A mixture of HL (25.4 mg, 0.1 mmol), NaOH (4.0 mg, 0.1 mmol), and $Pb(NO_3)_2$ (33.1 mg, 0.1 mmol) in 10 mL water was sealed in the autoclave at 180°C for 3 days. Colorless block crystals were obtained by filtration and washed with water and ethanol several times with a yield of 47%. Anal. Calcd for $C_{52}H_{45}N_{16}O_{13}Pb_2$ (%): C, 41.19; H, 2.99; N, 14.78. Found (%): C, 41.13; H, 3.07; N, 14.72. Main IR (KBr, cm^{-1}): 3440(vs, br), 1599(s), 1554(s), 1438(m), 1370(s), 1250(m), 1145(w), 1111(m), 1069(s), 1010(w), 920(w), 878(w), 831(w), 754(m), 725(m), 673(w), 657(w).

2.2.2. $[Ni(L)_2(H_2O)_2] \cdot 2H_2O$ (2). Complex **2** was obtained by the same procedure used for the preparation of **1** except that $Ni(NO_3)_2 \cdot 6H_2O$ (29.1 mg, 0.1 mmol) was used instead of $Pb(NO_3)_2$ as starting material. Green block crystals were obtained by filtration and washed with water and ethanol several times with a yield of 38%. Anal. Calcd for $C_{26}H_{26}N_8NiO_8$ (%): C, 49.01; H, 4.11; N, 17.58. Found (%): C, 49.07; H, 4.03; N, 17.63. Main IR (KBr, cm^{-1}): 3408(vs, br), 1568(s), 1511(m), 1415(s), 1352(s), 1288(m), 1212(m), 1050(s), 831(w), 769(w), 725(w), 616(w).

2.3. *X-ray structure determination*

Crystallographic data collections for **1** and **2** were carried out on a Bruker Smart Apex CCD area-detector diffractometer with graphite-monochromated Mo-Kα radiation ($\lambda = 0.71073$ Å) at 293(2) K using the ω-scan technique. Diffraction data were integrated by the SAINT program [13], which was also used for intensity corrections for Lorentz and polarization effects. Semi-empirical absorption correction was applied using SADABS [14]. The structures were solved by direct methods and all non-hydrogen atoms were refined anisotropically on F^2 by full-matrix least-squares using the SHELXL-97 crystallographic software package [15]. Hydrogens of L^- in **1** and **2** were generated geometrically, while those of water are located directly. Details of the crystal parameters, data collection, and refinements for **1** and **2** are summarized in table 1. Selected bond lengths and angles for **1** and **2** are listed in table 2. The hydrogen bonding data are given in table 3.

3. Results and discussion

3.1. *Description of the crystal structure of 1*

X-ray crystallographic analysis revealed that **1** crystallizes in the monoclinic space group *C2/c*, with two different Pb(II) atoms in the asymmetric unit (table 1, figure 1a). Both Pb1 and Pb2 sit on specific positions. Each Pb1 is six-coordinate by two imidazole nitrogens (N7, N7A) and four carboxylate oxygens (O1, O2, O1A, O2A) from four different L^-. The bond distances of Pb1–N7, Pb1–O1, and Pb1–O2 are 2.467(6), 2.580(5), and 2.765(6) Å, respectively, and the coordination angles around Pb1 are in

Table 1. Crystal data and structure refinements for **1** and **2**.

	1	**2**
Empirical formula	$C_{52}H_{45}N_{16}O_{13}Pb_2$	$C_{26}H_{26}N_8NiO_8$
Formula weight	1516.42	637.26
Temperature (K)	293(2)	293(2)
Crystal system	Monoclinic	Triclinic
Space group	*C2/c*	$P\overline{1}$
Unit cell dimensions (Å, °)		
a	17.941(2)	7.1745(10)
b	14.8140(17)	9.0322(12)
c	19.677(2)	10.7183(14)
α	90	73.765(2)
β	97.554(2)	87.008(1)
γ	90	78.299(2)
Volume (Å^3), *Z*	5184.3(10), 4	653.00(15), 1
Absorption coefficient (mm^{-1})	6.571	0.812
D_c (g cm^{-3})	1.943	1.620
F(000)	2948	330
θ range for data collection (°)	1.99–25.25	1.98–25.25
Reflections collected	12,911	3330
Independent reflections	3662	2120
Goodness-of-fit	0.946	1.045
Final *R* indices $[I>2\sigma(I)]^{a,b}$	$R_1=0.0389$, $wR_2=0.0898$	$R_1=0.0304$, $wR_2=0.0812$
R indices (all data)	$R_1=0.0500$, $wR_2=0.0934$	$R_1=0.0326$, $wR_2=0.0822$
Data/restraints/parameters	4685/0/380	2314/0/212
Largest difference peak and hole (e Å^{-3})	2.065 and −1.243	0.352 and −0.299

[a] $R_1=\Sigma||F_o|-|F_c||/\Sigma|F_o|$; [b] $wR_2=|\Sigma w(|F_o|^2-|F_c|^2)|/\Sigma|w(F_o)^2|^{1/2}$, where $w=1/[\sigma^2(F_o^2)+(aP)^2+bP]$, $R_2=(F_o^2+2F_c^2)/3$.

Table 2. Selected bond lengths (Å) and angles (°) for **1** and **2**.

1			
Pb1–O1	2.580(5)	Pb1–N7	2.467(6)
Pb1–O2	2.765(6)	Pb2–O3#1	2.636(5)
Pb2–O5	2.432(8)	Pb2–O4#1	2.746(5)
Pb2–N3	2.587(6)		
O1–Pb1–O2	48.27(16)	O1–Pb1–N7#3	77.10(18)
O1–Pb1–N7	81.02(18)	O2–Pb1–N7	84.12(18)
O1–Pb1–O1#3	147.9(2)	O2–Pb1–O2#3	139.72(17)
O1–Pb1–O2#3	148.87(16)	O2–Pb1–N7#3	125.12(18)
O5–Pb2–N3	71.66(14)	N7–Pb1–N7#3	93.3(3)
O3#1–Pb2–O5	83.79(12)	O3#3–Pb2–N3	76.57(17)
O4#3–Pb2–O5	113.41(13)	O3#1–Pb2–O4#1	48.21(16)
O3#1–Pb2–N3	99.45(18)	O3#1–Pb2–O3#3	167.6(2)
O4#1–Pb2–N3	74.43(18)	O4#1–Pb2–N3#2	121.22(17)
N3–Pb2–N3#2	143.3(3)	O3#3–Pb2–O4#1	138.79(16)
O4#1–Pb2–O4#3	133.2(3)		
2			
Ni1–O3	2.1038(14)	Ni1–N1	2.0985(14)
Ni1–N3#4	2.0878(15)		
O3–Ni1–N1	89.09(6)	O3–Ni1–O3#6	180.0
O3–Ni1–N3#4	87.22(6)	O3–Ni1–N1#6	90.91(6)
O3–Ni1–N3#5	92.78(6)	N1–Ni1–N3#4	87.07(6)
N1–Ni1–N3#5	92.93(6)	N3#4–Ni1–N3#5	180.0
N1–Ni1–N1#6	180.0		

Symmetry transformations used to generate equivalent atoms: #1 $x, y, -1+z$; #2 $-x, y, -1/2-z$; #3 $-x, y, 1/2-z$; #4 $x, y, 1+z$; #5 $-x, 2-y, 1-z$; #6 $-x, 2-y, 2-z$.

Table 3. Hydrogen bonding distances (Å) and angles (°) for **1** and **2**.

D–H···A	d(H···A)	d(D···A)	∠(D–H···A)
1			
O5–H5C···N5#1	2.0600	2.878(8)	160
O6–H6C···O1#2	1.9800	2.827(9)	172
O7–H7C···O2#3	2.1000	2.943(10)	171
O7–H40···O3	2.25(10)	2.849(9)	139(10)
2			
O4–H111···O1#4	2.20(3)	2.858(3)	156(4)
O4–H112···O1#5	2.05(4)	2.784(3)	155(4)
O3–H113···O2#6	1.90(3)	2.708(2)	161(3)
O3–H114···O2#7	2.02(3)	2.795(2)	163(3)

Symmetry transformations used to generate equivalent atoms: #1 $1/2-x, 1/2+y, 1/2-z$; #2 $1/2+x, 1/2+y, z$; #3 $x, 1-y, 1/2+z$; #4 $1-x, 1-y, 1-z$; #5 $x, 1+y, z$; #6 $-1+x, 1+y, z$; #7 $-x, 1-y, 2-z$.

the range 48.27(16)–148.87(16)° (table 2). Each Pb2 is seven-coordinate by two imidazole nitrogens [N3, N3C with Pb2–N3 = Pb2–N3C = 2.587(6) Å], four carboxylate oxygens [O3A, O4A, O3B, O4B, Pb2–O3A = Pb2–O3B = 2.636(5) Å, Pb2–O4A = Pb2–O4B = 2.746(5) Å] from four distinct L$^-$, and an additional oxygen [O5, Pb2–O5 = 2.432(8) Å] from a terminal water. Coordination angles around Pb2 are in the range 48.21(16)–167.6(2)° (table 2). Each L$^-$ connects two Pb(II) atoms to form an infinite 1-D double chain using one imidazole and a carboxylate in chelating coordination, while another imidazole of L$^-$ is uncoordinated (figure 1b).

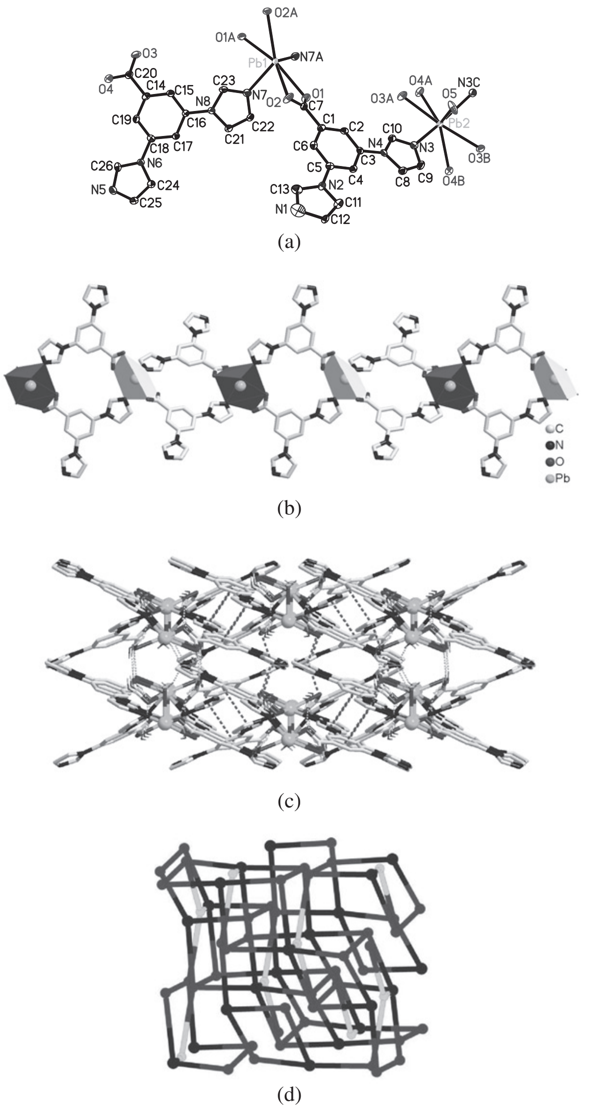

Figure 1. (a) The coordination environment of Pb(II) in **1** with ellipsoids drawn at the 30% probability level. The hydrogens and free water are omitted for clarity. (b) 1-D double chain in **1**. (c) 3-D structure of **1** linked by hydrogen bonds (thin dotted lines) and π–π interactions (thick dotted lines). (d) The simplified topological representation of the 3-D supramolecular architecture of **1**.

There are different kinds of π–π interactions in the packing diagram of **1** [16, 17]. One is between the central benzene and an adjacent imidazole ring with centroid to centroid distance of 3.54 Å and dihedral angle of 5.12°; the others are between imidazole rings with centroid to centroid distances of 3.71 and 3.67 Å and dihedral angles of 9.78 and 6.65°, respectively, as illustrated in figure 1(c). Such π–π interactions further link the 1-D chains to form a 3-D structure. Furthermore, the uncoordinated imidazoles in the chain form O–H $\cdots$ N hydrogen bonds with coordinated water from an adjacent chain, and the carboxylate groups in the chains form O–H $\cdots$ O hydrogen bonds with lattice water (table 3). These hydrogen bonds consolidate the 3-D framework of **1** (figure 1c). Topological analysis was carried out for the 3-D structure of **1** calculated by using the TOPOS software [18]. According to the simplification principle, each Pb1 and Pb2 can be viewed as four- or five-connected nodes, respectively [19]. Two different L^-, one coordinated (O5), and two free water molecules (O6, O7) can be considered as three-, four-, three-, two-, and two-connected nodes, respectively. Such connectivity repeats infinitely to give the 3-D framework of **1** as schematically shown in figure 1(d). The resulting structure of **1** is an unprecedented penta-nodal (3,4,5)-connected net with its Point (Schläfli) symbol of $(4 \cdot 6^2 \cdot 8 \cdot 10^2)_2(4 \cdot 6^2)_2(4^2 \cdot 6^4 \cdot 8^2 \cdot 10^2)(4^2 \cdot 6^4)(8^2 \cdot 10)$.

3.2. *Description of the crystal structure of 2*

When $Ni(NO_3)_2 \cdot 6H_2O$, instead of $Pb(NO_3)_2$, was taken into the reaction with HL and NaOH, a new coordination polymer **2** with different structure was isolated. X-ray crystallographic analysis reveals that **2** crystallizes in triclinic space group $P\overline{1}$ (table 1). The Ni1 sitting on the inversion center is six-coordinate with a distorted octahedral coordination geometry by four nitrogens (N1, N1A, N3B, N3C) from four different L^- ligands and two oxygens (O3 and O3A) from two terminal waters (figure 2a). The bond distances and angles around Ni1 (table 2) are in the normal range compared with previously reported Ni(II) complexes [20]. Each L^- links two Ni(II)'s to form an infinite 1-D double strand chain (figure 2b). Although each L^- is a μ_2-bridge in both **1** and **2**, the uncoordinated groups of L^- are different, an imidazole in **1** and carboxylate in **2**.

The π–π interaction between the central benzene and an adjacent imidazole ring with a centroid to centroid distance of 3.69 Å and dihedral angle of 9.40° is found, which links the 1-D chains to a 2-D layer (figure 2c). The coordinated and uncoordinated waters form O–H $\cdots\cdot$ O hydrogen bonds with the carboxylate of L^-, further extending 2-D layers to a 3-D framework (table 3 and figure 2d). Similar topological analysis was carried out for **2**; each Ni(II), L^-, coordinated and uncoordinated water can be regarded as six-, five-, three-, and two-connected nodes, respectively. Such connectivity repeats infinitely to give the 3-D framework of **2** as schematically shown in figure 2(e). The resulting structure of **2** is an unprecedented tri-nodal (3, 5, 6)-connected net with its Point (Schläfli) symbol of $(4 \cdot 6^2)_2(4^2 \cdot 5^2 \cdot 6^8 \cdot 7^2 \cdot 10)(4^2 \cdot 5^5 \cdot 6^3)_2$.

A large number of Pb(II) and Ni(II) complexes based on N and O coordination donor ligands have been reported till now, and the complexes show diverse structures since the Pb(II) or Ni(II) have varied coordination geometries and the N and O donor ligands have different coordination modes [21–30]. It is noteworthy that L^- has non-coordinated imidazole or carboxylate in **1** and **2**, leading to the formation of 1-D chains through coordination interactions.

3.3. *Thermogravimetric analysis and photoluminescent property*

The TGA were performed to investigate the thermal stabilities of the complexes, and the results are shown in figure 3. Complex **1** shows a weight loss of 5.67% from 100°C to 130°C corresponding to the release of coordinated and free water (Calcd 5.94%); further decomposition of the residue occurred at 320°C. For **2**, the weight loss starts at *ca* 165°C with the liberation of uncoordinated and coordinated water resulting in a

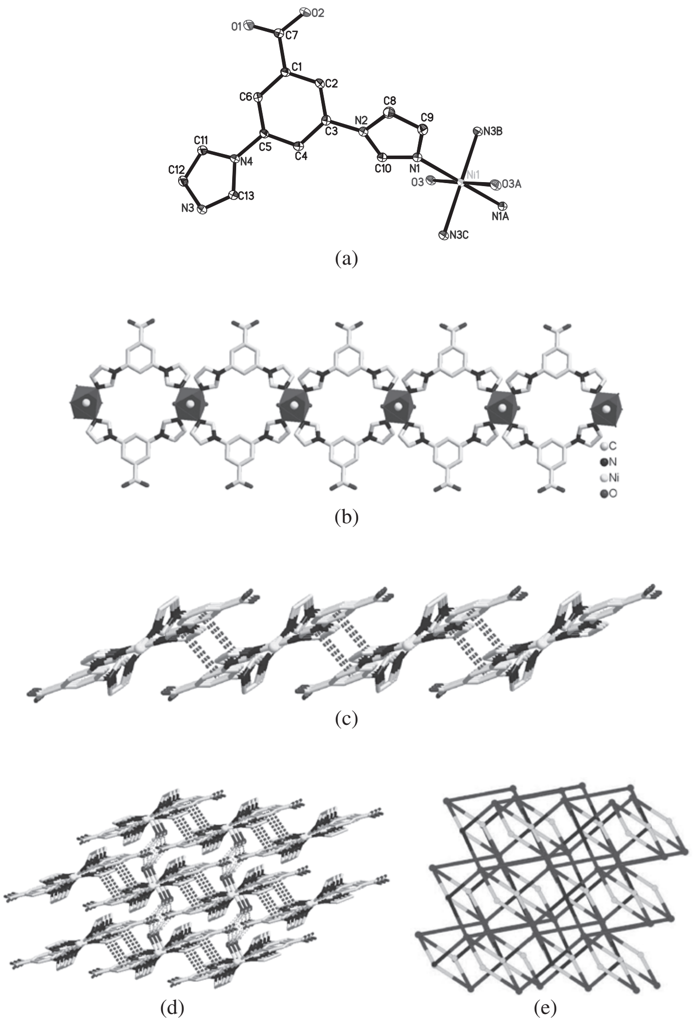

Figure 2. (a) The coordination environment of Ni(II) in **2** with the ellipsoids drawn at the 30% probability level. Hydrogens and uncoordinated water are omitted for clarity. (b) 1-D double chain in **2**. (c) 2-D network in **2** linked by π–π interactions. (d) 3-D structure of **2** linked by hydrogen bonds indicated by dashed lines. (e) The simplified topological representation of 3-D supramolecular architecture of **2**.

weight loss of 10.87% (Calcd 11.28%); decomposition of the residue was observed at 265°C. The results indicate that the complexes with the same ligands but different metal centers have different stability.

Photoluminescence of HL, **1** and **2** were studied in the solid state at room temperature under the same experimental conditions and all measurements of emission spectra were excited at a wavelength of 360 nm. As shown in figure 4, emission bands were observed at 460 and 520 nm for **1**, whereas no clear luminescence was detected for **2** or free HL. The emission bands of **1** may be assigned to metal to ligand charge transfer (MLCT) with electrons being transferred from lone pair of Pb(II) to the unoccupied π^* orbital of HL [31, 32].

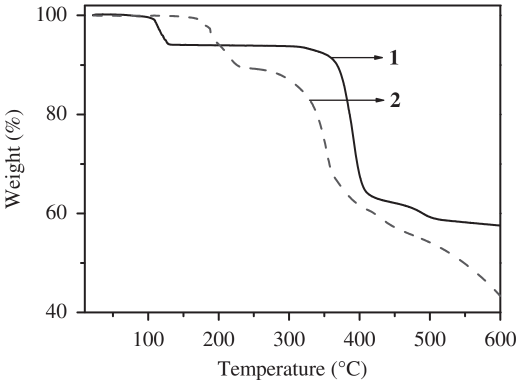

Figure 3. The TG curves of **1** and **2**.

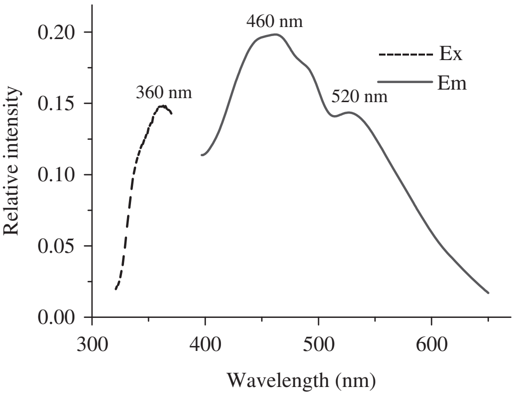

Figure 4. The excitation and emission spectra of **1**.

Supplementary material

Crystallographic data for the structures reported in this article have been deposited with the Cambridge Crystallographic Data Centre as Supplementary Publication No. CCDC-785663 and 785664. Copies of the data can be obtained at http://www.ccdc.cam.ac.uk/conts/retrieving.html (or from the CCDC, 12 Union Road, Cambridge CB2 1EZ, UK; Fax: +44 1223336033; Email: deposit@ccdc.cam.ac.uk).

Acknowledgments

This work was supported by the National Natural Science Foundation of China (Grant Nos. 20731004 and 20721002) and the National Basic Research Program of China (Grant Nos 2007CB925103 and 2010CB923303).

References

[1] G. Férey. *Chem. Soc. Rev.*, **37**, 191 (2008).
[2] J. Lee, O.K. Farha, J. Roberts, K.A. Scheidt, S.T. Nguyen, J.T. Hupp. *Chem. Soc. Rev.*, **38**, 1450 (2009).
[3] M. Kurmoo. *Chem. Soc. Rev.*, **38**, 1353 (2009).
[4] M.D. Allendorf, C.A. Bauer, R.K. Bhakta, R.J.T. Houk. *Chem. Soc. Rev.*, **38**, 1330 (2009).
[5] J.R. Li, R.J. Kuppler, H.C. Zhou. *Chem. Soc. Rev.*, **38**, 1477 (2009).
[6] J. Fan, L. Gan, H. Kawaguchi, W.Y. Sun, K.B. Yu, W.X. Tang. *Chem. Eur. J.*, **9**, 3965 (2003).
[7] L. Hou, J.P. Zhang, X.M. Chen, S.W. Ng. *Chem. Commun.*, 4019 (2008).
[8] C.D. Ene, A.M. Madalan, C. Maxim, B. Jurca, N. Avarvari, M. Andruh. *J. Am. Chem. Soc.*, **131**, 4586 (2009).
[9] Y. Yan, X. Lin, S.H. Yang, A.J. Blake, A. Dailly, N.R. Champness, P. Hubberstey, M. Schröder. *Chem. Commun.*, 1025 (2009).
[10] X.D. Chen, X.H. Zhao, M. Chen, M. Du. *Chem. Eur. J.*, **15**, 12974 (2009).
[11] Z. Su, K. Cai, J. Fan, S.S. Chen, M.S. Chen, W.Y. Sun. *CrystEngComm*, **12**, 100 (2010).
[12] Z. Su, Z.S. Bai, J. Xu, T.-A. Okamura, G.X. Liu, Q. Chu, X.F. Wang, W.Y. Sun, N. Ueyama. *CrystEngComm*, **11**, 873 (2009).
[13] *SAINT*, Version 6.2, Bruker AXS, Inc., Madison, WI (2001).
[14] G.M. Sheldrick. *SADABS*, University of Göttingen, Göttingen, Germany (1997).
[15] G.M. Sheldrick. *SHELXTL*, Version 6.10, Bruker Analytical X-ray Systems, Madison, WI (2001).
[16] S.Y. Wan, Y.Z. Li, T.-A. Okamura, J. Fan, W.Y. Sun, N. Ueyama. *Eur. J. Inorg. Chem.*, 3783 (2003).
[17] S.Y. Wan, J. Fan, T.-A. Okamura, H.F. Zhu, X.M. Ouyang, W.Y. Sun, N. Ueyama. *Chem. Commun.*, 2520 (2002).
[18] V.A. Blatov. *TOPOS, A Multipurpose Crystallochemical Analysis with the Program Package*, Samara State University, Russia (2004).
[19] A.T. Balaban. *From Chemical Topology to Three-Dimensional Geometry*, Plenum Press, New York (1997).
[20] S.T. Zheng, J. Zhang, J.M. Clemente-Juan, D.Q. Yuan, G.Y. Yang. *Angew. Chem. Int. Ed.*, **48**, 7176 (2009).
[21] I.S. Evstifeev, M.A. Kiskin, V.S. Mironov, A.S. Bogomyakov, A.A. Sidorov, V.M. Novotorstsev, I.L. Ermenko. *Inorg. Chem. Commun.*, **13**, 498 (2010).
[22] A. Aslani, A. Morsali, M. Zeller. *Solid State Sci.*, **10**, 1591 (2008).
[23] J. Fan, Y.A. Zhang, T.-A. Okmura, Z.H. Zou, N. Ueyama, W.Y. Sun. *Inorg. Chem. Commun.*, **4**, 501 (2001).
[24] M.L. Hu, Y.P. Lü, H.M. Zhang, B. Tu, Z.M. Jin. *Inorg. Chem. Commun.*, **9**, 962 (2006).
[25] K.Y. Choi, H. Ryu, Y.M. Lim, N.D. Sung, U.S. Shim, M. Suh. *Inorg. Chem. Commun.*, **6**, 412 (2003).
[26] H. Haddadian, A. Aslani, A. Morsali. *Inorg. Chim. Acta*, **362**, 1805 (2009).
[27] Z.R. Ranjbar, A. Morsali. *J. Mol. Struct.*, **936**, 206 (2009).
[28] M.J.S. Fard-Jahromi, A. Morsali. *Ultrason. Sonochem.*, **17**, 435 (2010).
[29] X.H. Miao, L.G. Zhu. *Inorg. Chim. Acta*, **361**, 2828 (2008).
[30] M. Payehghadr, S. Yousefi, A. Morsali. *J. Organomet. Chem.*, **693**, 2514 (2008).
[31] B. Xu, Z.G. Guo, H.X. Yang, G.L. Li, T.F. Liu, R. Cao. *J. Mol. Struct.*, **922**, 140 (2009).
[32] B. Wu, Z.G. Ren, H.X. Li, M. Dai, D.X. Li, Y. Zhang, J.P. Lang. *Inorg. Chem. Commun.*, **12**, 1168 (2009).